Downregulation of Retinal Connexin 43 in GFAP-Expressing Cells Modifies Vasoreactivity Induced by Perfusion Ocular Pressure Changes

Guodong Liu,[1,2] Hui Li,[1,2] Grant Cull,[2] Laura Wilsey,[2] Hongli Yang,[2] Jesica Reemmer,[3] Hai-Ying Shen,[3] Fang Wang,[1] Brad Fortune,[2] Bang V. Bui,[4] and Lin Wang[2]

[1]Department of Ophthalmology, Shanghai Tenth People's Hospital, Shanghai, China
[2]Devers Eye Institute, Legacy Research Institute, Portland, Oregon, United States
[3]RS Dow Neurobiology, Department of Translational Neuroscience, Legacy Research Institute, Portland, Oregon, United States
[4]Department of Optometry and Vision Sciences, University of Melbourne, Parkville, Victoria, Australia

Correspondence: Lin Wang, Devers Eye Institute, Legacy Health, 1225 NE 2nd Ave, Portland, OR, 97232, USA;
lwang@deverseye.org.

Received: July 31, 2020
Accepted: December 18, 2020
Published: January 27, 2021

Citation: Liu G, Li H, Cull G, et al. Downregulation of retinal connexin 43 in GFAP-expressing cells modifies vasoreactivity induced by perfusion ocular pressure changes. *Invest Ophthalmol Vis Sci.* 2021;62(1):26. https://doi.org/10.1167/iovs.62.1.26

Purpose. Glia and their communication via connexin 43 (Cx43) gap junctions are known to mediate neurovascular coupling, a process driven by metabolic demand. However, it is unclear whether Cx43 mediated glial communication intermediates classical autoregulation. Here we used viral transfection and a glial fibrillary acidic protein (GFAP) promoter to downregulate glial Cx43 to evaluate its role in retinal vascular autoregulation to ocular perfusion pressure (OPP) reduction.

Methods. Adult rats were intravitreally injected with the viral active construct or a control. Three weeks after the injection, eyes were imaged using confocal scanning laser ophthalmoscopy before and during a period of OPP decrease induced by blood draw to lower blood pressure or by manometric IOP elevation. Vessel diameter responses to the OPP decrease were compared between Cx43-downregulated and control-injected eyes. The extent of Cx43 downregulation was evaluated by Western blot and immunohistochemistry.

Results. In control eyes, the OPP decrease induced dilatation of arterioles, but not venules. In Cx43-downregulated eyes, Cx43 expression in whole retina was decreased by approximately 40%. In these eyes, the resting diameter of the venules increased significantly, but there was no effect on arterioles. In Cx43-downregulated eyes, vasoreactivity evoked by blood pressure lowering was significantly compromised in both arterioles ($P = 0.005$) and venules ($P = 0.001$). Cx43 downregulation did not affect the arteriole responses to IOP elevation, whereas the responses of the venules showed a significantly greater decrease in diameter ($P < 0.001$).

Conclusions. The downregulation of retinal Cx43 in GFAP–expressing cells compromises vasoreactivity of both arterioles and venules in response to an OPP decrease achieved via blood pressure lowering or IOP elevation. The results also suggest that Cx43-mediated glial communication actively regulates resting venular diameter.

Keywords: ocular perfusion pressure, connexin 43, Adeno-Associated Virus, retinal vasculature, autoregulation

Glia are the most abundant cells in the central nervous system, where they undertake tasks that support normal neuronal physiology. Their range of activities includes maintaining homeostasis of extracellular ions and neurotransmitters, participation in glucose metabolism, and in metabolic waste removal.[1–3] Glia also play a critical role in regulating local blood flow in response to changes in neuronal and subsequent metabolic activity in both brain[4,5] and retina,[6,7] a feedforward process known as neurovascular coupling, which is the basis of functional magnetic resonance imaging.

Glia, and more specifically astrocytes, have been demonstrated to mediate vascular tone[8,9] and tone-dependent vascular responses to a variety of stimuli in the brain.[10] We previously demonstrated that perivascular glia in rat retina were activated in response to acute IOP elevation, as evidenced by increased intracellular calcium concentration.[11] Pharmacologic inhibition of glial activity significantly blunted calcium activation and impaired the capacity for the vasculature to respond to IOP elevation. This finding is consistent with the results of Kim et al.,[9] which showed that the inhibition of astrocyte activation (decreased calcium

activity) attenuated compensatory vascular responses to an acute, phenylephrine-induced elevation of the systemic blood pressure (BP). Collectively, these results support the novel idea that glia are engaged in pressure-initiated classic blood flow autoregulation.

Autoregulation is an intrinsic feature of certain tissues whereby blood flow is optimized to rapidly adapt to changes in perfusion pressure and metabolic demands. In regard to the eye, ocular perfusion pressure (OPP) is defined as the difference between the mean arterial BP and the IOP. Given that a change in either of those pressures can impact transmural pressure, one might expect the glia to modulate the vascular responses to BP-lowering as they are known to do during IOP elevation.[11] Thus, a key aim of this study is to compare the effect of glial cells on retinal vascular responses to a decreased OPP achieved via IOP elevation or an equivalent decrease in the BP. Because both IOP elevation and BP lowering decrease the OPP and have been considered to be risk factors for glaucoma,[12,13] the results may help to better define the vasopathology of glaucoma and other diseases.

Connexin 43 (Cx43) is a subunit protein of gap junctions,[14] which facilitate astrocytic intercellular communication and their communication with mural cells.[15–19] In the retina, Cx43 is expressed predominantly within the perivascular endfeet of astrocytes[20] and has been functionally associated with vascular regulation.[21] Indeed, the intravitreal injection of a pharmacologic Cx43 inhibitor (Gap27) caused significant attenuation of the optic nerve blood flow response to IOP elevation in rabbit eyes.[22] However, Cx43 has also been localized to the retinal pigment epithelium, Müller cells, and some neurons in rat retina.[20,23] Thus, the effect of pharmacologic inhibition may not be specific for glial cells.

An alternate approach is to target Cx43 downregulation using a glial cell specific promoter. In our previous studies in brain,[24,25] we used an adeno-associated viral vector (AAV) to upregulate adenosine kinase with an astrocytic-specific promoter in brain. Using a similar approach here, we designed an AAV8 vector combined with *GFAP* gene promoter and corresponding microRNA (miRNA) to downregulate Cx43 in retinal glia.[26] We test the hypothesis that glial cell gap junction communication modulates pressure-induced vascular responses (i.e., classical autoregulation) in rat retina.

Specifically, we examined the impact of modifying glial cell communication on the autoregulatory responses of arterioles and venules. In the retina, venules do not have smooth muscle cells and are thus thought to be passively regulated. However, recent experimental evidence shows that isolated retinal venules exhibit constriction and dilation in response to the local delivery of vasoactive substances,[27] thus suggesting the existence of active regulatory mechanism(s) as well. We previously showed that the pharmacologic inhibition of glial activity increased the basal venular diameter and compromised the responses of both the arterioles and the venules to a rapid increase in the IOP.[11] These data are consistent with the possibility that glial cells participate in the maintenance of both basal venular tone and the regulation of vascular resistance in response to changes in the local pressure environment. However, the rapid IOP elevation used in our previous study can introduce an abrupt compression of the vessels, which may complicate interpretation. As such, a slower change in the OPP may be better for revealing active contributions of glia to vascular regulation. To consider this possibility, here we examined the impact of downregulating Cx43 on vascular responses to a slower OPP reduction.

Methods

Animals

Adult male Brown Norway rats (Charles River Laboratories Inc., Wilmington, MA), weighing an average of 322 ± 70 g, were maintained under a 12-hour light/12-hour dark cycle (1200 lux maximum, <100 lux inside the cage) with normal rat chow and water available ad libitum. All experimental methods and animal care procedures conformed to the National Institutes of Health guidelines for the care and use of Laboratory animals and the ARVO Statement. All experiments were approved by the Legacy Institutional Animal Care and Use Committee.

Two groups of rats were intravitreally injected with an AAV delivery system containing either an active miRNA to downregulate Cx43 expression in the retinal glia (experimental group) or a scrambled control miRNA (control group) as detailed elsewhere in this article. Three weeks after the injection, arteriolar and venular vasoreactivity in response to either slow IOP elevation ($n = 8$ each for the Cx43 downregulated group and the control group) or BP lowering ($n = 8$ each for the Cx43 downregulated group and control group) was evaluated by measuring vessel diameter during OPP reduction in vivo. The arteriolar and venular responses were compared between the Cx43 downregulated and control groups. After euthanasia, the efficiency of Cx43 downregulation was evaluated by Western blot analysis and immunohistochemistry. The procedures are detailed elsewhere in this article.

Preparation of the Cx43 AAV Construct

Aiming to downregulate Cx43 in retinal cells expressing GFAP, an AAV system was used to deliver the corresponding miRNA using a *GFAP* promoter. The viruses are recombinant AAVs containing a cassette from serotype 2 packaged in the capsid from serotype 8. AAV8 capsid was selected owing to its particular effectiveness in driving transgene expression in glia and in particular astrocytes.[28] The expression of Cx43 was downregulated using AAV2/8 vectors encoding a miRNA targeting the rat *Cx43* gene under a full-length *GFAP* promoter (AAV.GFAP. miRNACx43). The miRNA constructs were designed with sense and antisense "pin" regions separated by a loop region. Post-transcriptional regulatory element WPRE and polyA elements were also included. The miRNA sequence was: TAGGAAGAGAAGC-TAAACAAATGC, which is complementary to the native Cx43 miRNA for the purpose of decreasing translational efficiency. For the control virus, the cassette bore a scrambled miRNA sequence, which was designed not to have viable base pairing with any genes in this species, with otherwise matching promoter and enhancing elements to the experimental virus (AAV.GFAP.miRNAScramble). WPRE and polyA elements were used.

For in-house viral production, human embryonic kidney 293T cell lines were maintained in Dulbecco's modified Eagle's Medium supplemented with 10% FBS and 100 U/mL penicillin-streptomycin (Gibco, Thermo Fisher Scientific Inc., Waltham, MA) at 37 °C and with 5% CO_2. Cells were passaged into 150-mm plates (Corning Inc., Corning, NY) 1 day before transfection and triple transfected at

Investigative Ophthalmology & Visual Science

approximately 70% confluency using PEI Max 40K following the manufacturer's recommended protocol. For each transfection, 7.5 µg of pAR8 AAV8 serotype packaging plasmid, 10 µg of pDF6 helper plasmid, and 5 µg of AAV plasmid carrying the construct of interest were added to 500 µL of Dulbecco's modified Eagle's Medium. Next, 90 µL of PEI "Max" solution (1 mg/mL, pH of 7.4) was added to the mixture and incubated at room temperature for 5 to 10 minutes. After incubation, the mixture was added to 15 mL of warm maintenance media freshly added in each dish 2 hours prior. Cells were harvested between 48 hours and 72 hours after transfection by scraping and the viruses were crudely isolated from the cell membranes via freeze–thaw cycling and centrifugation. The AAV2/8 (AAV2 ITR vectors pseudo-typed with AAV8 capsid) viral particles were then purified from the supernatant via discontinuous iodixanol gradient (protocol by Addgene, Watertown, MA). All dosages of AAV were adjusted with sterile phosphate buffered saline (Gibco, Grand Isle, NY) before in vivo injection. For each eye, 3 to 4 µL of 10^{13} virus genomes per milliliter AAV.GFAP.Cx43miRNA (Cx43 downregulated group) or corresponding control (AAV.GFAP.miRNA.Scramble) was injected. The injection was repeated 3 days later.

The viral transfection was confirmed by encoding a gene of jellyfish green fluorescent protein (GFP) (AAV8.GFAP.GFP) in three rat eyes after a single intravitreal injection. Colocalization of GFP and GFAP was examined in isolated retina immunohistochemically stained with antibodies to GFAP and GFP (to amplify its fluorescent signal).

Anesthesia and Surgical Preparation

Three weeks after the first intravitreal injection, animals underwent general anesthesia induced via isoflurane inhalation (1.5% to 2.5% in oxygen at a flow rate of 1–2 mL/min). Both femoral arteries and veins were cannulated with polyethylene tubing (PE10 or 50; BD Intramedic, Franklin Lakes, NJ). One femoral artery was connected to a pressure transducer (BLPR2; World Precision Instruments or WPI, Sarasota, FL) and a four-channel amplifier system (LabTrax-4/24T; WPI) for continuous BP monitoring. A femoral vein was used for administration of maintenance anesthetic. The other artery or vein was used for blood drawing to lower the BP during the experiments (discussed elsewhere in this article). After these surgical preparations, anesthesia was switched to continuous intravenous infusion of sodium pentobarbital (2–5 mg/kg/h, Nembutal, Oak Pharmaceuticals, Lake Forest, IL) via an infusion pump (Aladdin, World Science Instruments). An orotracheal intubation was performed allowing the animal to be ventilated with approximately 30% O_2 (RSP 1002 ventilator, Kent Scientific Co., Torrington, CT) and the end tidal carbon dioxide partial pressure was monitored with a capnometry (RSP-300, Kent Scientific Co.). The respiratory rate (60–90 stroke/min), the peak inspiratory pressure and inspiration/expiration ratio were adjusted to maintain an arterial partial pressure of carbon dioxide ($PaCO_2$) between 30 and 40 mm Hg, which was periodically measured using a blood gas analyzer (i-STAT, Abbott Inc., Princeton, NJ). A calibration curve between the $PaCO_2$ and end tidal carbon dioxide partial pressure was established based on 27 measurements in 12 animals, which allowed the continuously monitored end tidal carbon dioxide partial pressure to be used as a surrogate for $PaCO_2$ throughout subsequent experiments. Arterial partial pressure of oxygen throughout all procedures was more than 100 mm Hg. Pupils were dilated with topical application of tropicamide (0.5%, Alcon Laboratories Inc., Fort Worth, TX). Body temperature was maintained between 37 °C and 38 °C with a thermostatically controlled heating pad. Custom-made rigid gas-permeable contact lenses (3.5 mm posterior radius of curvature, 5.0 mm optical zone diameter, and +5.0 diopter back vertex power) were used to maintain clarity during ocular fundus imaging.

Retinal Vessel Diameter Imaging and Quantification

Rats were placed in a prone position on a stage facing a confocal scanning laser ophthalmoscope (Spectralis OCT+HRA, Heidelberg Engineering, Heidelberg, Germany). At baseline and during BP lowering or IOP elevation, video sequences (5 Hz acquisition) in infrared reflectivity mode (confocal scanning laser infrared imaging) were recorded across a 30° field centered on the optic nerve head. Reactivity in vessel diameter induced by a change in OPP was quantified offline using Fiji (ImageJ v2.0.0; National Institutes of Health, Bethesda, MD),[29] an open-source platform for biological image analysis. In brief, 10 consecutive images were averaged to return a single image every 2 seconds. Averaged images recorded immediately before and during OPP modification were combined into a single image stack. This image stack was registered with custom software written in Java to allow the same regions of interest to be analyzed across time. Regions of interest were selected along arterioles and venules at 1 disc diameter distance from the optic disc margin (Fig. 1A).

In each retina, the vessel diameter was measured from three to five arterioles and three to five venules. The coefficient of variation of 10 sequential baseline vessel diameter measurements from confocal scanning laser infrared images was 1.27% for arterioles and 1.62% for venules ($n = 17$ eyes).

The change in the diameter of each vessel was expressed as a percentage relative to its own baseline. Data obtained during the course of each experiment were averaged into 10-mm Hg OPP bins. The OPP was calculated as the difference between mean arterial BP and IOP.

Gradual OPP Reduction by BP Lowering and IOP Elevation

To lower BP, blood was drawn from a femoral vein or artery with a syringe pump at a rate of 0.8 to 1.0 mL/min. Blood drawing started when the mean BP had stabilized between 95 and 100 mm Hg under pentobarbital anesthesia. To induce a gradual increase in the IOP, a 33G needle connected to a reservoir filled with balanced salt solution (BSS, Baxter, Deerfield, IL) was inserted into the anterior chamber. IOP was set to 10 mm Hg as a baseline level. The reservoir was then raised at a rate of 0.16 ± 0.05 mm Hg/sec using a pulley driven by a modified peristaltic pump (Longer Precision Pump Co., Ltd, Hebei, China). The final target IOP elevation was confirmed using a rebound tonometer (TONO-LAB, Vantaa, Finland).

Experimental Protocol

After completion of the surgical preparation, time was allowed for the BP to stabilize between 95 and 100 mm

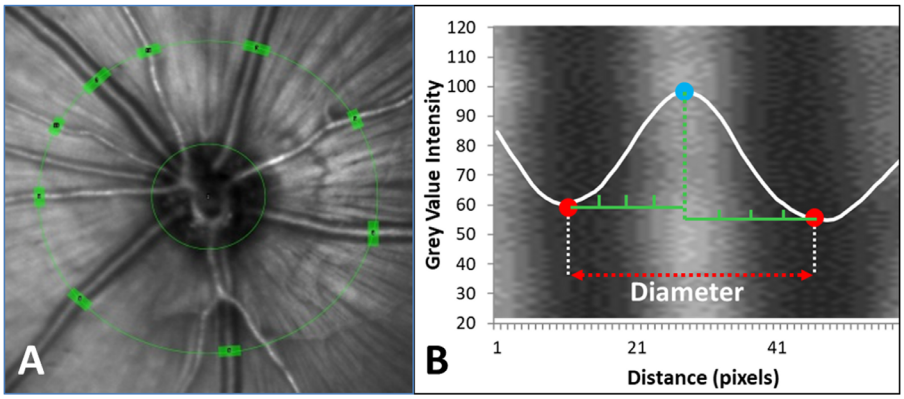

Figure 1. Peripapillary vessel diameter measurement from confocal scanning laser infrared images. (**A**) Images of the ocular fundus recorded by confocal scanning laser infrared. (**B**) Using ImageJ, the reflectance intensity profile across each vessel (*white line*) was generated and analyzed for peak (*blue*) and troughs (*red*). Vessel diameter (*red dashed line*) was defined as the distance between 2 troughs perpendicular to the vessel axis.

Hg and $PaCO_2$ to stabilize between 30 and 40 mm Hg. Once stabilized a 20-second baseline confocal scanning laser infrared image sequence was acquired, followed by continuous imaging (5 frames per second) during the period of OPP modification until BP decreased to 20 to 30 mm Hg or IOP increased to 70 mm Hg. The net OPP change was approximately 60 mm Hg over the course of 4 to 6 minutes in both groups. Changes in vessel diameter were compared between Cx43 downregulated and control eyes during BP and IOP manipulation ($n = 8$ for each experimental condition). The effect of IOP elevation on the vessel diameter was also assessed in a group of naïve eyes (without any treatment, $n = 8$).

Western Blot Analysis for Cx43

To evaluate the efficiency of Cx43 downregulation, 4 additional pairs of Cx43 downregulated eyes and control eyes were used. At the same endpoint (3 weeks after injection) the retina was isolated and as much of the vitreous as possible was removed. Tissues were then immediately lysed in RIPA buffer (50 mM pH 7.5 Tris, 150 mM NaCl, 1% Triton X-100, 0.5%SDS, 1% sodium deoxycholate, protease inhibitor cocktail) for 1 hour on ice, then homogenized in a sonicator at 15% amplitude for 10 seconds. Total protein concentration was determined using the BCA protein assay kit (Thermo Scientific Inc.). Lysate protein (20 µg) was subjected to 8% to 16% SDS-PAGE (Bio-Rad, Hercules, CA) transferred onto polyvinyl difluoride membranes (PVDF, Bio-Rad), blocked with 5% nonfat milk for 1 hour and incubated with rabbit anti-Cx43 antibody (1:1,000, Cell Signaling, Danvers, MA) at 4 °C overnight. After three washes in TBS-T (0.1% Tween-20 in TBS), the blots were incubated with HRP-conjugated secondary antibody (1:10000, Cell Signaling) for 1 hour. The membranes were exposed (Immun-Star Chemiluminescent Protein Detection System; Bio-Rad) using an enhanced chemiluminescence detection kit (Thermo Scientific Inc.).

The membranes were washed and blocked with 5% nonfat milk, incubated with rabbit anti-GAPDH antibody (1:5000, ab9485, Abcam, Cambridge, MA) and secondary antibody. Membranes were then imaged as described elsewhere in this article and a densitometric analysis was performed using ImageJ.

Immunohistochemical Evaluation of Cx43 Expression

Three weeks after the first injection and after imaging, rats were perfusion fixed with transcardial infusion of 4% paraformaldehyde. The retinas were isolated for cross-sections ($n = 4$) and flat mounts ($n = 4$). For the cross-sections, eyes were embedded in optimal cutting temperature compound (Electron Microscopy Science, Hatfield, PA) and sectioned at 10 to 12 µm thickness. Sections were rinsed three times in PBS for 5 minutes, incubated in Triton X-100 (0.3%) for 15 minutes at room temperature and then in blocking serum (5% goat serum and 5% BSA) for 1 hour. A chicken primary antibody to GFAP (1:1000; Sigma-Aldrich Corp., St Louis, MO) and a rabbit primary antibody to Cx43 (1:400; Cell Signaling, Danvers, MA) were applied overnight at 4 °C. After three PBS washes, sections were incubated with goat anti-chicken and goat anti-rabbit secondary antibodies conjugated with AlexaFluor 488 and 555 (1:400 and 1:200; Life Technologies), respectively, for 1 hour at room temperature.

For flat mount retinas, similar immunohistochemistry procedures were followed, except that a greater concentration of Triton X-100 (1%) was used. The primary antibodies were incubated for 2 days and the secondary antibodies were incubated overnight, both at 4 °C. A confocal microscope (DMi8, Confocal system TCSSPE; Leica, Wentzler, Germany) was used to evaluate the retinas.

Data Analysis and Statistics

The effect of OPP lowering (binned every 10 mm Hg) on the relative change in vessel diameter was analyzed using one-way repeated measures ANOVA (1-way ANOVA) with Dunnett's post hoc comparisons at each OPP level. To evaluate the effect of Cx43 downregulation, the relative change in the vessel diameter as a function of OPP was compared between the Cx43 downregulated and the control groups using 2-way ANOVA (OPP and Cx43 downregulation) separately for BP-lowering and IOP elevation experiments. Paired *t* tests or Wilcoxon matched-pairs signed rank tests as appropriate were used to evaluate differences between groups. The probability (*P*) to reject the null hypothesis was set at 5%. Data are shown as mean ± SD unless

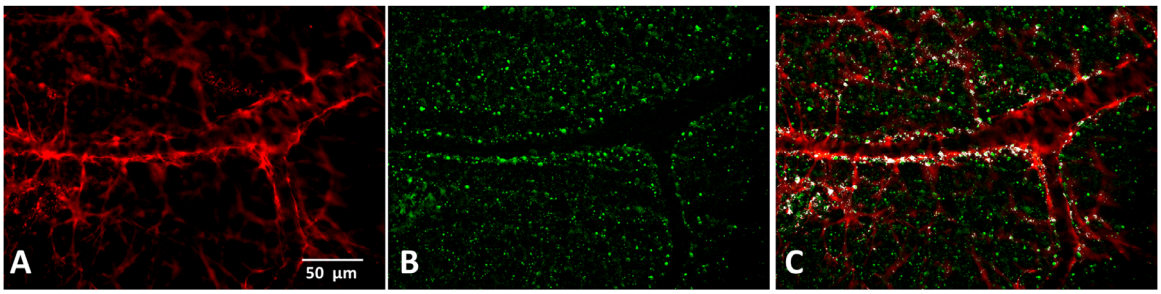

Figure 2. Representative microphotograph of GFP expression and GFAP immunoreactivity in rat retina 3 weeks after intravitreal injection of AAV8.GFAP.GFP. (**A**) At the center of the image is a horizontally oriented vessel. GFAP-positive cells and their processes line the vessel wall. (**B**) Immunohistochemically enhanced GFP expression appears as punctate distribution. (**C**) Costain of GFAP and GFP shows strong overlap between GFP and GFAP (scale bar: 50 µm).

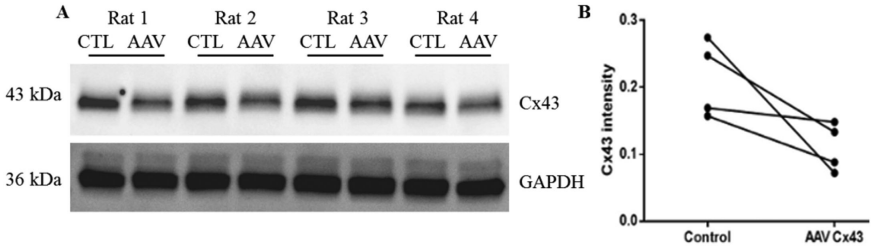

Figure 3. Expression of Cx43 determined by Western blot in 4 pairs of retinas. (**A**) Each pair of lanes shows the immunoblots for Cx43 and GAPDH from the same rat treated with AAV.GFAP.miRNACx43 (AAV) and control. (**B**) Relative Cx43 concentration in each pair of retinas quantified by using ImageJ.

otherwise specified. All analyses were performed using Prism 7 (GraphPad Software, Inc., La Jolla, CA).

Results

GFAP Promoter Controlled GFP Transduction in GFAP-Positive Cells

Figure 2 shows an example of the GFP and GFAP immunohistochemical staining in a flat-mount retina 3 weeks after AAV8.GFAP.GFP injection. The majority of the GFP immunoreactivity is co-localized with that of GFAP positive cells alongside the vessel walls.

Western Blot Quantification of Retinal Cx43

Figure 3 shows the results of Western blot analysis in four pairs of eyes treated with AAV.GFAP.Cx43miRNA or control (Fig. 3A). The Cx43 protein level in the Cx43 downregulated eyes was 40 ± 2.0% lower than the control eyes (Fig. 3B, $P = 0.06$, paired Wilcoxon test).

Expression of Cx43 by Immunofluorescence Staining

Figures 4 and 5 show two pairs of representative retinas of whole mount and cross-sections, respectively. In whole-mounted control retinas, Cx43 was evident as densely distributed puncta, primarily co-localized with GFAP-positive cells (Fig. 4C). Cross-sections showed that Cx43 puncta were limited to the inner retinal layers (retinal ganglion cell and nerve fiber layers) of the retina. In Cx43 downregulated retinas, glia were structurally disorganized with increased GFAP expression (Fig. 4D). Cross-sections showed GFAP immunoreactivity extending radially into the inner retinal layers (Fig. 5). This pattern is consistent with activated Müller cells (Fig. 5D). There were few Cx43-positive puncta in Cx43 downregulated eyes. An occasional puncta could be found, but these were smaller in size compared with the control eyes.

Basal Vessel Diameter Difference Between the Cx43 Downregulated and Control Groups

In rats assigned to BP lowering, the average basal arteriolar diameter (by pixel) was 19.8 ± 1.8 in the control group and 21.4 ± 2.5 in the Cx43 downregulated group ($P = 0.17$, unpaired t test) three weeks after AAV construct injection. The corresponding venular diameter was 24.2 ± 2.5 and 29.3 ± 3.2 in the control and Cx43 downregulated groups ($P = 0.003$), respectively. Note that, under similar conditions of image acquisition previously, we found that each pixel corresponds to 1.6 µm across adult rat retina.[30,31]

In rats assigned to IOP elevation, the average basal arteriolar diameter was 22.2 ± 1.8 in the control group and 24.6 ± 4.6 in the Cx43 downregulated group ($P = 0.21$). The venular diameter was 28.5 ± 4.9 and 39.2 ± 6.9 in the control and Cx43 downregulated groups ($P = 0.007$), respectively. Thus, in both experimental groups, the basal diameter of the venules was significantly increased as a result of Cx43 downregulation.

Investigative Ophthalmology & Visual Science

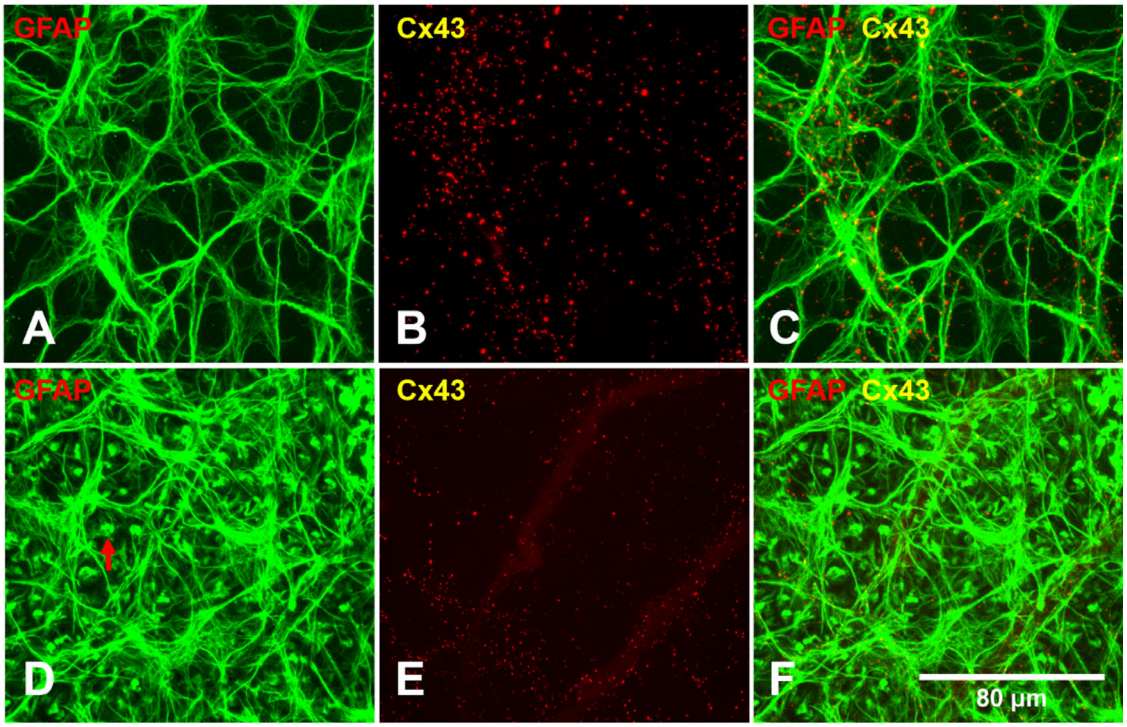

Figure 4. Representative GFAP and Cx43 staining in whole-mounted retinas from an AAV.Cx43 downregulated eye and a control eye. In the control eye (**A–C**), the Cx43 puncta were colocalized with GFAP positive glia. In the Cx43 downregulated eye (**D–F**), GFAP immunoreactivity was enhanced and its pattern was disorganized (*arrow* in **D**). (**E**) Cx43 immunoreactivity appeared weaker and puncta were smaller. (**F**) Colocalization of **D** and **E**.

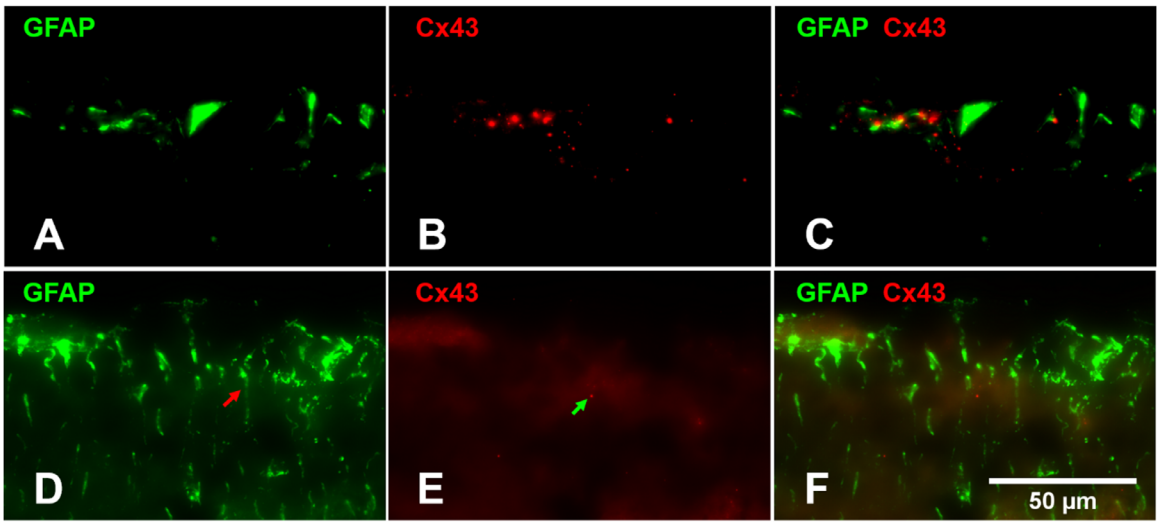

Figure 5. Representative GFAP (*green*) and Cx43 (*red*) staining in retinal cross sections (vitreal side up) from a control eye (**A–C**) and a Cx43 downregulated eye (**D–F**). In the control eye, GFAP staining and Cx43 puncta were colocalized and distributed in the superficial retinal layers. In Cx43 downregulated eyes, enhanced GFAP immunoreactivity was evident in both superficial and deeper retinal layers (**D**), whereas Cx43 puncta were smaller and fewer (**E**).

The Effect of Cx43 Downregulation on BP-Lowering Induced Vascular Responses

In rats assigned to BP lowering, the average OPP before the onset of BP reduction was 86.9 ± 3.2 mm Hg in the control group and 88.4 ± 2.9 mm Hg in the Cx43 downregulated group ($P = 0.30$, unpaired t test). After blood had been drawn, the BP was reduced by 72.5 ± 5.1 mm Hg and 69.8 ± 14.0 mm Hg ($P = 0.61$) in the control and Cx43 downregulated groups, respectively. The average blood volume drawn was 7.6 ± 1.1 mL and 6.8 ± 1.0 mL in the control and Cx43 downregulated groups ($P = 0.15$), respectively.

Investigative Ophthalmology & Visual Science

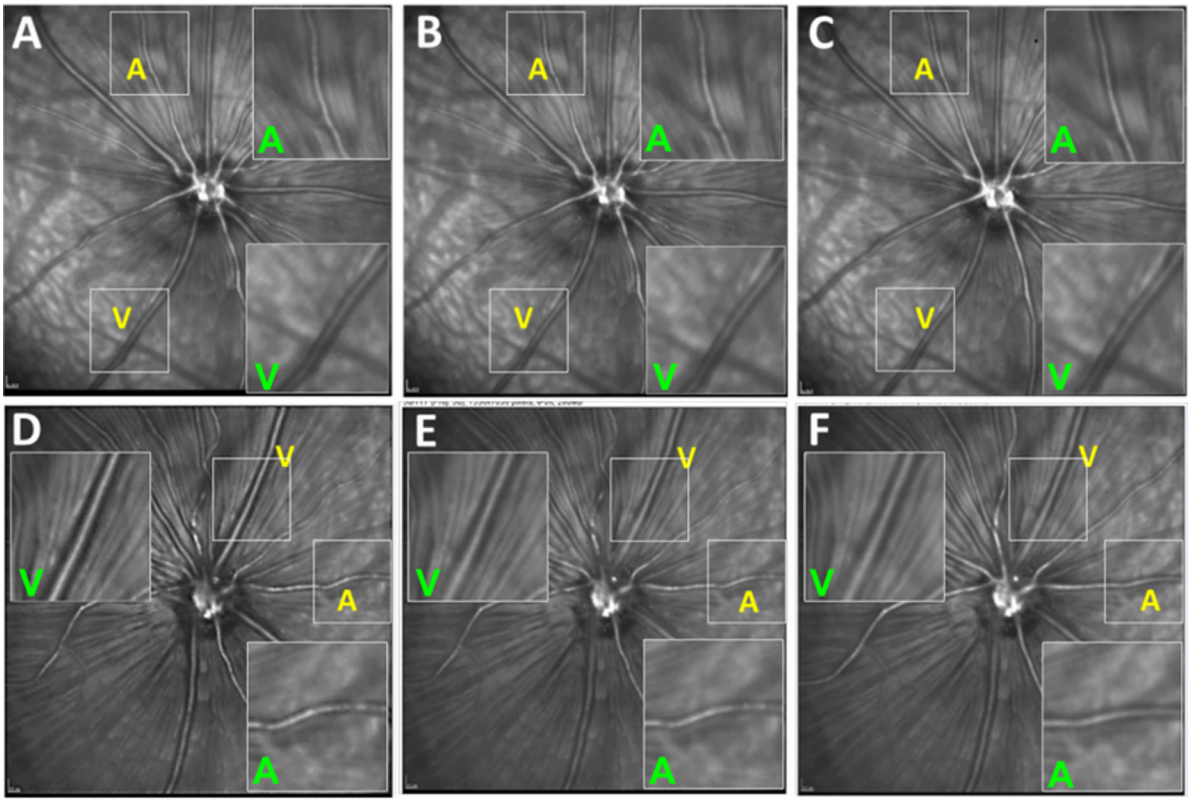

Figure 6. Confocal scanning laser images during BP reduction in a control eye (**A**–**C**) and a Cx43 downregulated eye (**D**–**F**) at baseline (**A**, **D**), 50 sec (**B**, **E**) and 100 sec after onset of OPP reduction by blood withdrawal (**C**, **F**). In the representative control eye, the arterioles (**A**) show mild dilation during BP-lowering while the venules (*V*) showed no change qualitatively. In the Cx43 downregulated eye, while arterioles dilated, the venules constricted. Note the larger venular diameter at baseline in the Cx43 downregulated eye compared with the control eye (**A** vs. **D**). In each image, the inset shows a portion of a selected arteriole and venule to provide a magnified view of the vessels.

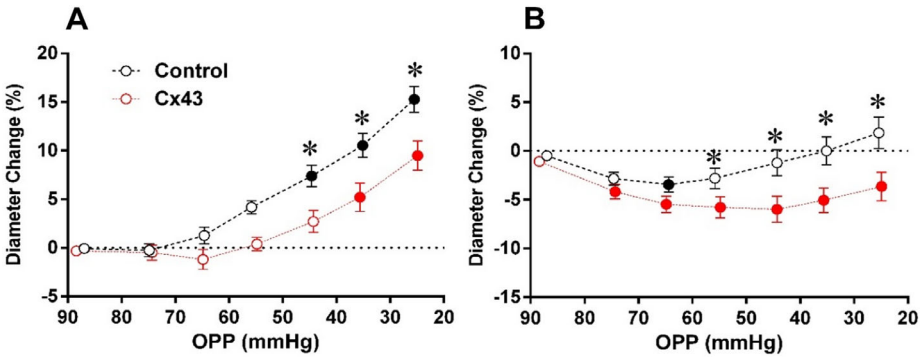

Figure 7. Effect of Cx43 downregulation on retinal arteriolar and venular diameter in responses to BP reduction. The relative change in arteriolar (**A**) and venular (**B**) diameter from baseline in control (*black*, $N = 8$) and Cx43 downregulated (*red*, $N = 8$) groups are plotted against OPP, summarized into 10-mm Hg bins. *Filled circles* indicate significant difference from baseline (the first symbol of each curve). Asterisks (*) indicate significant differences between the groups at given OPPs. (Error bar: SEM.)

The BP decreased at similar rates in the control and Cx43 downregulated groups as determined by linear regression (–0.27 mm Hg per second, $P = 0.69$, F test). The average baseline $PaCO_2$ was 32.2 ± 1.3 and 33.8 ± 3.0 mm Hg in the control and Cx43 downregulated groups, respectively ($P = 0.31$). The $PaCO_2$ during BP lowering in three separate experiments was 40.9 ± 8.1, 39.9 ± 7.7, 38.9 ± 6.8, and 38.6 ± 7.4 mm Hg measured when the BP was 90, 60, 50, and 40 mm Hg, respectively. Thus, the experimental conditions were similar for the Cx43 downregulated and control groups.

Figure 6 shows representative confocal scanning laser images from a control eye and a Cx43 downregulated eye. The vascular diameter change in these two eyes is close to the median level of their corresponding experimental groups. Group data are shown in Figure 7.

In the control eyes, as OPP was lowered to approximately 75 mm Hg via BP reduction, the arteriolar diameter started

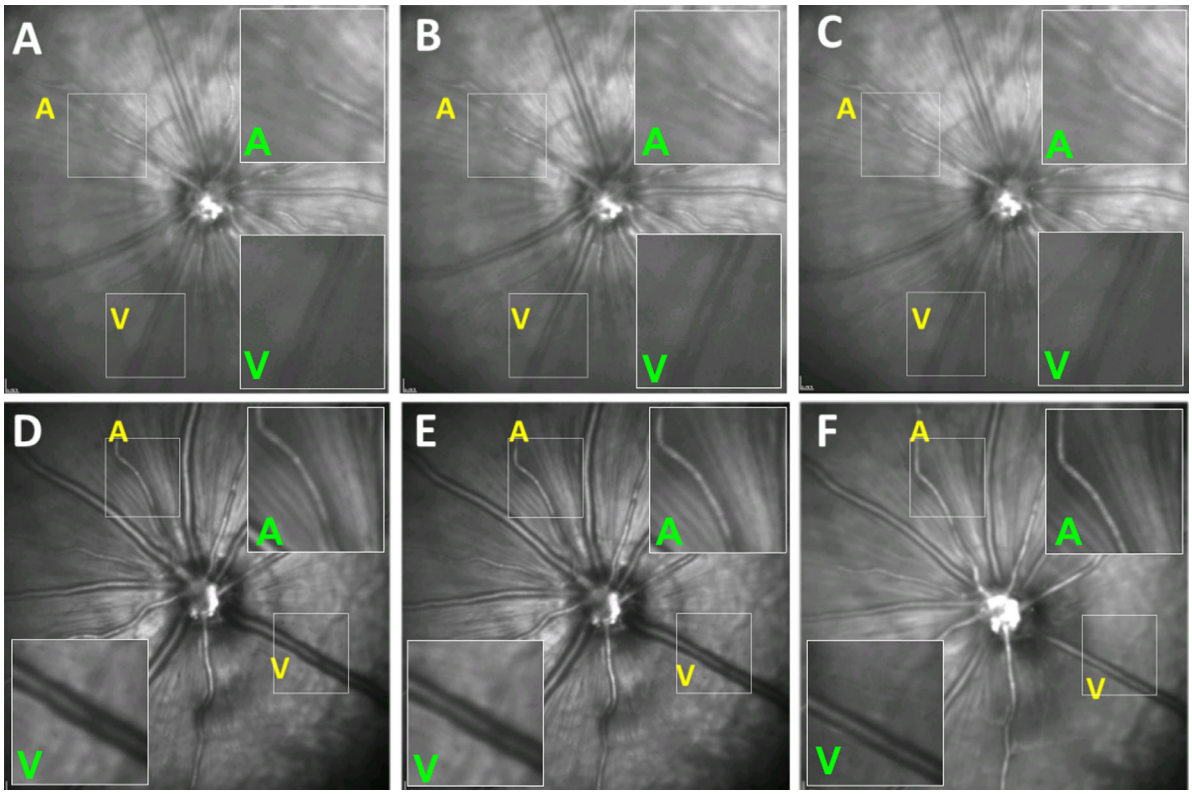

Figure 8. Representative confocal scanning laser images during IOP elevation in a control eye (**A–C**) and a Cx43 downregulated eye (**D–F**) before (**A**, **D**), 50 sec (**B**, **E**) and 100 sec (**C**, **F**) after IOP elevation. In the control eye, the arterioles (*A*) slightly dilated and the venules (*V*) slightly constricted during IOP elevation (**A–C**). In the Cx43 downregulated eye, arterioles dilated but the venules showed marked constriction. In each image, the *insets* show a portion of a selected arteriole and venule to provide a magnified view of the changes.

to dilate (Fig. 7A). Further OPP reduction to approximately 45 mm Hg caused a significant increase in the diameter, achieving an approximate 15% increase above baseline when the OPP reached 20 mm Hg (one-way ANOVA, $P < 0.0001$). In the Cx43 downregulated group, arterioles exhibited significantly less dilation compared with the control group ($P = 0.005$, two-way ANOVA). There was no significant increase in diameter detected until OPP had decreased to less than 40 mm Hg (Fig. 7A).

For venules (Fig. 7B), the OPP decrease in the control group caused a decrease in diameter, but the change was significant only at an OPP of 65 mm Hg ($P < 0.05$, –3% from baseline with a 95% CI from 0.11% to 5.80%). In the Cx43 downregulated group, there was a greater decrease in the venular diameter, with OPP lowering achieved via BP reduction (one-way ANOVA, $P < 0.0001$). The decrease in the venular diameter peaked at an OPP of 40 mm Hg. Further decreases in the OPP did not result in an additional decrease in the venular diameter. Compared with control eyes, the decrease in the venular diameter in the Cx43 downregulated group to less than 60 mm Hg of OPP was statistically significant ($P = 0.001$, two-way ANOVA).

Effect of Cx43 Downregulation on IOP-Induced Vascular Responses

The average OPP at the start of the IOP elevation experiment was 87.2 ± 3.7 mm Hg in control and 89.2 ± 2.3 mm Hg in the Cx43 downregulated groups ($P = 0.17$, unpaired *t* test). Figure 8 shows representative confocal scanning laser images from a control and a Cx43-downregulated eye.

The vessel diameter changes as a function of OPP are summarized in Figure 9. In control eyes, gradually decreasing the OPP by increasing the IOP from 10 to 70 mm Hg induced a progressive increase in arteriolar diameter ($P < 0.0001$, one-way ANOVA) after an initial small decrease. In the Cx43 downregulated eyes, the magnitude of the arteriolar diameter increase tended to be slightly larger than that observed in control eyes, but the difference did not achieve statistical significance ($P = 0.68$, two-way ANOVA, Fig. 9A).

For venules, IOP elevation caused only an approximately 5% decrease in the diameter in control eyes but a significant vasoconstriction of approximately 15% in Cx43 downregulated eyes ($P < 0.0001$). This decrease in the venule diameter was significantly greater compared with the control eyes (Fig. 9B, $P = 0.001$, two-way ANOVA).

Vasoreactivity to IOP Elevation in Naïve Eyes

To address a potential off-target Cx43 transduction in smooth muscle cells, the arteriolar diameter responses in Cx43 downregulated and control eyes during IOP elevation were compared against naïve control eyes. Fig. 9A shows that the vascular responses in the naïve eyes (blue symbols and lines) were not significantly different from the other two groups ($P = 0.64$, ANOVA).

Investigative Ophthalmology & Visual Science

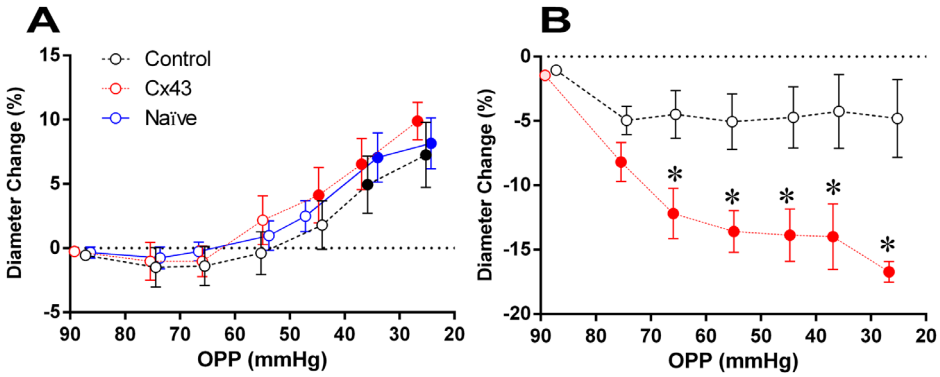

Figure 9. Effect of Cx43 downregulation on retinal arteriolar and venular diameter responses to IOP elevation. Change in arteriolar (**A**) and venular (**B**) diameter relative to baseline in control (*black*, $N = 8$) and Cx43 downregulated (*red*, $n = 8$) groups, plotted against OPP averaged into 10-mm Hg bins. *Filled circles* indicate a significant difference from baseline. Asterisks (*) indicate significant difference between the control and Cx43 downregulated groups at a given level of OPP. (Error bar: SEM.) The *blue curve* (*left panel*) represents the arteriolar diameter responses in the group of naïve eyes (*blue*, *solid lines*).

Discussion

By using a viral delivery system to downregulate Cx43 in GFAP-expressing glial cells in the rat retina, our results show that glial communication via gap junctions plays a role in modulating the basal venular diameter and vasoreactivity to BP lowering in both the arterioles and venules and to IOP elevation in the venules.

It is known that decreasing the perfusion pressure drives arteriolar dilation to maintain an adequate blood flow.[32,33] Our data are consistent with this finding because they show arteriolar dilation in response to both BP lowering (Fig. 7A) and IOP elevation (Fig. 9A). Our data show that impairment of the Cx43-mediated communication compromised the vascular response to BP decreases for retinal arterioles by significantly decreasing the magnitude of their dilation.

Although the *GFAP* promoter will largely target GFAP-expressing retinal astrocytes, Müller cells, which express GFAP under stress or disease conditions,[26,34] may also be targeted under these conditions. Figure 4D shows an increased GFAP expression in clumps and puncta whose position is consistent with Müller cell processes, which are structurally and functionally connected closely with astrocytes.[35–37] Therefore, we cannot exclude the possibility that the effects on Müller cells may have also contributed to the altered vascular responses we observed after Cx43 downregulation, although how the Müller cells interact to regulate retinal circulation via Cx43 remains unknown.

In addition to glia, Cx43 is also found in pericytes, which have been shown to regulate blood flow in the capillaries via Cx43[38] and in smooth muscle cells in the arterioles.[39] Although, the activation of miRNA is controlled within GFAP-expressing cells, it is possible that our results reflect in part an off-target downregulation of Cx43. Our analysis has focused on changes to the diameter of larger vessels, rather than capillaries that may be impacted by altered pericyte communication. With regard to the off-target transduction of smooth muscle cells, we show that IOP-induced arteriolar responses in AAV control and Cx43 downregulated eyes were not different to naïve eyes. This finding suggests our treatment has not compromised the capacity for smooth muscle cells around arterioles to respond to increases in the IOP. Given this result, the significant impairments of vasodilation after Cx43 downregulation induced by BP lowering is unlikely to be impaired via changes in the contractility of smooth muscle cells.

It should be noted that, to achieve systemic hypotension, we used a controlled withdrawal of blood in this study, rather than using pharmacologically vasoactive agents. This approach produced a more gradual decrease in the BP and avoided potential off-target effects directly affecting local vasoreactivity. However, lowering the blood volume may decrease oxygen availability and the rate of metabolic waste removal, both of which may affect blood flow regulation.[40] To avoid these potential problems, animals were artificially ventilated and given 30% oxygen. We show that during blood withdrawal both the arterial partial pressure of oxygen and the $PaCO_2$ were not significantly altered from baseline.

In contrast with compromised dilation in response to BP lowering, the arteriolar response to gradual IOP elevation in Cx43 downregulated eyes was largely unaffected. This finding contrasts with the results of studies that used the gliotoxin aminoadipic acid glial inhibitor, in which the vascular responses to IOP elevation were significantly suppressed.[11,41] However, it should be noted that, in those studies, aminoadipic acid caused extensive glial cellular damage as evidenced by the near complete disappearance[11] or significantly suppression[35] of GFAP immunohistochemical reactivity. In eyes treated with AAV.GFAP.Cx43miRNA in this study, the glial cells appeared to remain present, albeit with slightly altered morphology and GFAP expression (Fig. 4D). In addition, the rate and amplitude of IOP elevation were quite different in those studies. In the current study, IOP was gradually increased from 10 to 70 mm Hg over the course of 5 to 6 minutes, whereas previously[11] the IOP was rapidly increased from 20 to 50 mm Hg within several seconds. Rapid increases in the IOP have been demonstrated to have a greater physical impact on blood flow compared with the same magnitude of IOP elevation achieved at a slower rate.[42,43] Thus, the downregulation of Cx43 activity may have a milder effect than the chemicals to allow arterioles retaining the capacity to efficiently respond to gradual IOP elevations.

Our data also show that Cx43 downregulation affected the arterioles differently when challenged with BP lowering or IOP elevation. Why this result might be the case is likely to be related to the difference in hemodynamic impact between BP lowering and IOP elevation. First, BP lowering

Investigative Ophthalmology & Visual Science

was induced by withdrawing blood. Blood volume reduction decreases shear stress, an important hemodynamic element maintaining basal vascular tone.[44] In contrast, an equivalent IOP elevation results in no change or only smaller decrease of shear stress. The work of Blanco et al[10] showed that, when the basal vascular tone was low (larger diameter), the activation of glia drove vasodilation. In contrast, when the basal vascular tone was higher (smaller diameter) activating glia induced vasoconstriction.[10] We speculate that BP lowering, which decreases shear stress and arterial tone, might lead to more glial activated to keep the vessel dilated compared with IOP elevation. This result may account for our observation that Cx43 downregulation impact arterial response to BP lowering (Fig. 7A) but not to IOP elevation (Fig. 9A). Another difference in the hemodynamics between the two approaches with regard to the venules is that the intravenous pressure kept increasing at a few millimeters of mercury higher than the IOP during IOP elevation,[45–47] whereas no change during BP elevation, although the net transmural pressure in the venules remains similar in both OPP challenges.

The current results support a possible role for glial cells in the active regulation of retinal venules. Retinal venules, which lack smooth muscle cells, are thought to passively regulate their diameter following the changes in OPP and blood volume. When the extravenous pressure or IOP increases, the venules are passively compressed and act like a collapsible tube, such that upstream vascular resistance is increased to maintain the venular pressure at levels slightly above the IOP, a mechanism known as the Starling effect.[48–50] The current results in control eyes with a IOP elevation show that the diameter of arterioles increased the venular diameter but decreased only slightly (5%). This outcome is an indication that the venular blood volume remained relatively stable owing to effective arteriolar autoregulation. However, in Cx43-downregulated eyes, the arteriolar response remained similar to that observed in control eyes, whereas the venular diameter following IOP elevation was sharply reduced (Fig. 9, *red curves*). This finding suggests that the venules are actively regulated by a mechanism that depends on intact gap junction communication by glial cells.

The idea that glial cells contribute to venular regulation is also supported by the significantly larger basal venular diameter (32%, $n = 28$), but no difference in arteriole diameter in Cx43 downregulated eyes. Similar diameter changes were observed in our previous study (33% larger) after glial cells were inhibited pharmacologically.[11] We also previously showed that autoregulation is decreased when the basal diameter is increased. Specifically, under hypercapnia, a decrease in the relative magnitude of vasodilation was associated a larger basal vessel diameter.[40] Because there was no change in the basal arteriolar diameter after Cx43 downregulation in this study, it is unlikely that the observed effect (Fig. 7A) arises from a change in the basal tone. In contrast, it is possible that the venules, having lost their basal tone, follow the Starling law[49] and behave more like a simple collapsible tube. Taken together, our data show that glial communication modifies the basal venular diameter as well as the vasoreactivity of the venules to an OPP challenge and thus support the conclusion that retinal venules are actively regulated by mechanisms involving intact communication by glial cells via their gap junctions.

This study has several limitations worthy of discussion. Although the viral delivery system using an AAV8 serotype has been reported to have high specificity for retinal astrocytes,[28,51] our Western blot results showed that there was approximately a 40% downregulation of the total retinal Cx43 protein compared with control eyes, suggesting incomplete Cx43 suppression. Although the immunohistochemical stains and protein analysis confirm the downregulation of Cx43, we do not have direct data to show that this change functionally impacts glial signaling. Further investigation is necessary to quantify the impact of Cx43 downregulation on communication between glia and blood vessels. Another consideration is that the vessel diameter is used here as a surrogate for the assessment of vascular autoregulation, rather than actual blood flow[52–54] or tissue oxygen extraction.[55] More subtle effects of inhibiting gap junction communication may be observed by measuring the changes in the blood flow specifically. Moreover, we also acknowledge that increasing the IOP may result in additional measurement error introduced by an increased axial length. However, we do not believe that changes in vessel diameter are due to this potential confound because the increase in the arteriolar diameter with BP lowering (Fig. 7A) was actually greater than that observed for IOP elevation (Fig. 9A). Further, there was no problem using the active eye tracking function of the confocal scanning laser instrument, which would have occurred if there were significant changes in lateral magnification.

In summary, this in vivo study using a viral delivery system to downregulate retinal Cx43 targeting GFAP expressing cells resulted a in significant modification of vasoreactivity to both BP- and IOP-induced OPP decreases. These results show that glial cells via Cx43 communication are involved in retinal vascular regulation in both arterioles and venules.

Acknowledgments

The authors thank Juan Reynaud and Zhongya Wang for technical assistance in imaging analysis and design of viral delivery system.

Supported by National Institute Health (R01-EY019939); Legacy Good Samaritan Foundation and Australian Research Council Future Fellowship.

Disclosure: **G. Liu**, None; **H. Li**, None; **G. Cull**, None; **L. Wilsey**, None; **H. Yang**, None; **J. Reemmer**, None; **H.-Y. Shen**, None; **F. Wang**, None; **B. Fortune**, None; **B.V. Bui**, None; **L. Wang**, None

References

1. de Hoz R, Rojas B, Ramirez AI, et al. Retinal macroglial responses in health and disease. *Biomed Res Int*. 2016;2016:2954721.
2. Gallo V, Chittajallu R. Unwrapping glial cells from the synapse: what lies inside? *Science*. 2001;292:872–873.
3. Haydon PG, Carmignoto G. Astrocyte control of synaptic transmission and neurovascular coupling. *Physiol Rev*. 2006;86:1009–1031.
4. Allen NJ, Barres BA. Neuroscience: glia - more than just brain glue. *Nature*. 2009;457:675–677.
5. Attwell D, Buchan AM, Charpak S, Lauritzen M, Macvicar BA, Newman EA. Glial and neuronal control of brain blood flow. *Nature*. 2010;468:232–243.
6. Newman EA. Glial cell regulation of neuronal activity and blood flow in the retina by release of gliotransmitters. *Phil Trans Roy Soc London B Biol Sci*. 2015;370:20140195.

7. Song Y, Nagaoka T, Yoshioka T, Nakabayashi S, Tani T, Yoshida A. Role of glial cells in regulating retinal blood flow during flicker-induced hyperemia in cats. *Invest Ophthalmol Vis Sci*. 2015;56:7551–7559.
8. Rosenegger DG, Tran CH, Wamsteeker Cusulin JI, Gordon GR. Tonic local brain blood flow control by astrocytes independent of phasic neurovascular coupling. *J Neurosci*. 2015;35:13463–13474.
9. Kim KJ, Iddings JA, Stern JE, et al. Astrocyte contributions to flow/pressure-evoked parenchymal arteriole vasoconstriction. *J Neurosci*. 2015;35:8245–8257.
10. Blanco VM, Stern JE, Filosa JA. Tone-dependent vascular responses to astrocyte-derived signals. *Am J Physiol Heart Circ Physiol*. 2008;294:H2855–2863.
11. Li H, Bui BV, Cull G, Wang F, Wang L. Glial cell contribution to basal vessel diameter and pressure-initiated vascular responses in rat retina. *Invest Ophthalmol Vis Sci*. 2017;58: 1–8.
12. Fechtner RD, Weinreb RN. Mechanisms of optic nerve damage in primary open angle glaucoma. *Surv Ophthalmol*. 1994;39:23–42.
13. Nicolela MT, Walman BE, Buckley AR, Drance SM. Ocular hypertension and primary open-angle glaucoma: a comparative study of their retrobulbar blood flow velocity. *J Glaucoma*. 1996;5:308–310.
14. Nielsen MS, Axelsen LN, Sorgen PL, Verma V, Delmar M, Holstein-Rathlou NH. Gap junctions. *Comprehensive Physiology*. 2012;2:1981–2035.
15. Escartin C, Rouach N. Astroglial networking contributes to neurometabolic coupling. *Front Neuroenerget*. 2013;5:4.
16. Pannasch U, Rouach N. Emerging role for astroglial networks in information processing: from synapse to behavior. *Trends Neurosci*. 2013;36:405–417.
17. Blomstrand F, Aberg ND, Eriksson PS, Hansson E, Ronnback L. Extent of intercellular calcium wave propagation is related to gap junction permeability and level of connexin-43 expression in astrocytes in primary cultures from four brain regions. *Neuroscience*. 1999;92:255–265.
18. Scemes E, Giaume C. Astrocyte calcium waves: what they are and what they do. *Glia*. 2006;54:716–725.
19. Leybaert L, Cabooter L, Braet K. Calcium signal communication between glial and vascular brain cells. *Acta Neurol Belg*. 2004;104:51–56.
20. Zahs KR, Kofuji P, Meier C, Dermietzel R. Connexin immunoreactivity in glial cells of the rat retina. *J Comp Neurol*. 2003;455:531–546.
21. Brisset AC, Isakson BE, Kwak BR. Connexins in vascular physiology and pathology. *Antioxid Redox Signal*. 2009;11:267–282.
22. Shibata M, Oku H, Sugiyama T, et al. Disruption of gap junctions may be involved in impairment of autoregulation in optic nerve head blood flow of diabetic rabbits. *Invest Ophthalmol Vis Sci*. 2011;52:2153–2159.
23. Danesh-Meyer HV, Zhang J, Acosta ML, Rupenthal ID, Green CR. Connexin43 in retinal injury and disease. *Prog Retin Eye Res*. 2016;51:41–68.
24. Shen HY, Sun H, Hanthorn MM, et al. Overexpression of adenosine kinase in cortical astrocytes and focal neocortical epilepsy in mice. *J Neurosurg*. 2014;120:628–638.
25. Theofilas P, Brar S, Stewart KA, et al. Adenosine kinase as a target for therapeutic antisense strategies in epilepsy. *Epilepsia*. 2011;52:589–601.
26. Lupien C, Brenner M, Guerin SL, Salesse C. Expression of glial fibrillary acidic protein in primary cultures of human Muller cells. *Exp Eye Res*. 2004;79:423–429.
27. Yu DY, Su EN, Cringle SJ, Morgan WH, McAllister IL, Yu PK. Local modulation of retinal vein tone. *Invest Ophthalmol Vis Sci*. 2016;57:412–419.
28. Aschauer DF, Kreuz S, Rumpel S. Analysis of transduction efficiency, tropism and axonal transport of AAV serotypes 1, 2, 5, 6, 8 and 9 in the mouse brain. *PLoS One*. 2013;8:e76310.
29. Schindelin J, Arganda-Carreras I, Frise E, et al. Fiji: an open-source platform for biological-image analysis. *Nat Methods*. 2012;9:676–682.
30. Abbott C, Choe T, Burgoyne C, Cull GA, Wang L, Fortune B. Comparison of retinal nerve fiber layer thickness in vivo and axonal transport after chronic intraocular pressure elevation in young versus older rats. *PLoS One*. 2014; 9:e114546.
31. Abbott CJ, Choe TE, Lusardi TA, Burgoyne CF, Wang L, Fortune B. Imaging axonal transport in the rat visual pathway. *Biomed Opt Exp*. 2013;4:364–386.
32. Schubert R, Mulvany MJ. The myogenic response: established facts and attractive hypotheses. *Clin Sci (Lond)*. 1999;96:313–326.
33. Guidoboni G, Harris A, Cassani S, et al. Intraocular pressure, blood pressure, and retinal blood flow autoregulation: a mathematical model to clarify their relationship and clinical relevance. *Invest Ophthalmol Vis Sci*. 2014;55:4105–4118.
34. Aartsen WM, van Cleef KW, Pellissier LP, et al. GFAP-driven GFP expression in activated mouse Muller glial cells aligning retinal blood vessels following intravitreal injection of AAV2/6 vectors. *PLoS One*. 2010;5:e12387.
35. Hollander H, Makarov F, Dreher Z, van Driel D, Chan-Ling TL, Stone J. Structure of the macroglia of the retina: sharing and division of labour between astrocytes and Muller cells. *J Comp Neurol*. 1991;313:587–603.
36. Zahs KR, Newman EA. Asymmetric gap junctional coupling between glial cells in the rat retina. *Glia*. 1997;20:10–22.
37. Zahs KR, Ceelen PW. Gap junctional coupling and connexin immunoreactivity in rabbit retinal glia. *Vis Neurosci*. 2006;23:1–10.
38. Alarcon-Martinez L, Villafranca-Baughman D, Quintero H, et al. Inter-pericyte tunneling nanotubes control local microvascular 4 dynamics and neurovascular coupling in vivo. *Nature*. 2020;585:91–95.
39. Yang G, Peng X, Wu Y, Li T, Liu L. Involvement of connexin 43 phosphorylation and gap junctional communication between smooth muscle cells in vasopressin-induced ROCK-dependent vasoconstriction after hemorrhagic shock. *Am J Physiol Cell Physiol*. 2017;313:C362–C370.
40. Liu G, Cull G, Wang L, Bui BV. Hypercapnia impairs vasoreactivity to changes in blood pressure and intraocular pressure in rat retina. *Optom Vis Sci*. 2019;96:470–476.
41. Shibata M, Sugiyama T, Kurimoto T, et al. Involvement of glial cells in the autoregulation of optic nerve head blood flow in rabbits. *Invest Ophthalmol Vis Sci*. 2012;53:3726–3732.
42. Riva CE, Hero M, Titze P, Petrig B. Autoregulation of human optic nerve head blood flow in response to acute changes in ocular perfusion pressure. *Graefes Arch Clin Exp Ophthalmol*. 1997;235:618–626.
43. Liang Y, Fortune B, Cull G, Cioffi GA, Wang L. Quantification of dynamic blood flow autoregulation in optic nerve head of rhesus monkeys. *Exp Eye Res*. 2010;90:203–209.
44. Henrion D. Pressure and flow-dependent tone in resistance arteries. Role of myogenic tone. *Arch Mal Coeur Vaiss*. 2005;98:913–921.
45. Morgan WH, Yu DY, Cooper RL, Alder VA, Cringle SJ, Constable IJ. Retinal artery and vein pressures in the dog and their relationship to aortic, intraocular, and cerebrospinal fluid pressures. *Microvasc Res*. 1997;53:211–221.
46. Attariwala R, Giebs CP, Glucksberg MR. The influence of elevated intraocular pressure on vascular pressures in the cat retina. *Invest Ophthalmol Vis Sci*. 1994;35:1019–1025.

Investigative Ophthalmology & Visual Science

47. Attariwala R, Glucksberg MR. Control mechanisms of retinal vein pressure: evaluation in the cat using an in situ infusion micropipette. *Microcirculation*. 1996;3:263–270.
48. Westlake WH, Morgan WH, Yu DY. A pilot study of in vivo venous pressures in the pig retinal circulation. *Clin Exp Ophthalmol*. 2001;29:167–170.
49. Simone RDE, Ranieri A, Bonavita V. Starling resistors, autoregulation of cerebral perfusion and the pathogenesis of idiopathic intracranial hypertension. *Panminerva Med*. 2017;59:76–89.
50. Kiel JW. *The Ocular Circulation*. San Rafael (CA): Morgan & Claypool Life Sciences; 2010.
51. Hammond SL, Leek AN, Richman EH, Tjalkens RB. Cellular selectivity of AAV serotypes for gene delivery in neurons and astrocytes by neonatal intracerebroventricular injection. *PLoS One*. 2017;12:e0188830.
52. O'Connell RA, Anderson AJ, Hosking SL, Bui BV. Provocative intraocular pressure challenge preferentially decreases venous oxygen saturation despite no reduction in blood flow. *Ophthalmic Physiol Opt*. 2015;35:114–124.
53. Zhi Z, Cepurna WO, Johnson EC, Morrison JC, Wang RK. Impact of intraocular pressure on changes of blood flow in the retina, choroid, and optic nerve head in rats investigated by optical microangiography. *Biomed Opt Express*. 2012;3:2220–2233.
54. Zhi Z, Cepurna W, Johnson E, Jayaram H, Morrison J, Wang RK. Evaluation of the effect of elevated intraocular pressure and reduced ocular perfusion pressure on retinal capillary bed filling and total retinal blood flow in rats by OMAG/OCT. *Microvasc Res*. 2015;101:86–95.
55. He Z, Lim JK, Nguyen CT, Vingrys AJ, Bui BV. Coupling blood flow and neural function in the retina: a model for homeostatic responses to ocular perfusion pressure challenge. *Physiol Rep*. 2013;1:e00055.

Investigative Ophthalmology & Visual Science